THE ASTROPHYSICAL JOURNAL, 437:560–563, 1994 December 20


# A MEDIUM-DEEP REDSHIFT SURVEY OF A MINISLICE AT THE NORTH GALACTIC POLE

C. N. A. WILLMER[1]
Observatório Nacional, Rua General José Cristino 77, 20921-030 Rio de Janeiro, RJ, Brazil;
and UCO/Lick Observatory, University of California

DAVID C. KOO[1]
UCO/Lick Observatory and Board of Studies in Astronomy and Astrophysics,
University of California, Santa Cruz, CA 95064

ALEX S. SZALAY[1]
Department of Physics, Johns Hopkins University, Homewood Campus, Baltimore, MD 21218;
and Department of Physics, Eötvös University, Budapest

AND

MICHAEL J. KURTZ
Harvard-Smithsonian Center for Astrophysics, 60 Garden Street, Cambridge, MA 02138
*Received 1994 March 14; accepted 1994 June 22*

## ABSTRACT

The first results from a new medium-deep redshift survey of galaxies in a 4° by 49′ slice close to the north Galactic pole have yielded 240 new redshifts, providing a total of 327 redshifts out of 814 galaxies visible to $B = 20$. This survey extends the transverse information for the first five peaks found in the redshift histogram from a deeper pencil beam sample reported by Broadhurst et al. The first peak, corresponding to the Great Wall, has a significant contribution from galaxies in the outer region of the Coma cluster. Another peak at $z \approx 0.125$ is largely confined to a small area and would have been missed by the original deep cone survey if the position were shifted by only 1° westward. Only one of the structures we detect has a wall-like appearance. In general, the high-density structures have irregular shapes, and alternate with low-density regions or voids with various sizes up to $\sim 100\ h^{-1}$ Mpc, which is a pattern similar to that detected by the shallower wide-angle surveys.

*Subject headings:* cosmology: observations — galaxies: clustering — galaxies: distances and redshifts

## 1. INTRODUCTION

In the analysis of a narrow-cone survey of faint field galaxies towards both Galactic poles, Broadhurst et al. (1990, hereafter BEKS) found that the redshift distribution showed a regular pattern of alternation between low- and high-density regions with a spacing of $\sim 128\ h^{-1}$ Mpc ($h = H_0/100$ km s$^{-1}$ Mpc$^{-1}$ and $q_0 = 0.5$ used throughout). The first peak in their northern sample corresponded to the Great Wall (hereafter GW; Geller & Huchra 1989). Because the scale size of the GW ($\sim 100\ h^{-1}$ Mpc) is larger than the characteristic depth of the nearby fully sampled surveys, very few of these features could have been detected (e.g., da Costa et al. 1988; Geller & Huchra 1989; Tully et al. 1992). Up to now only the GW has been studied in any detail (Ramella, Geller, & Huchra 1992, hereafter RGH; de Lapparent, Geller, & Huchra 1991, hereafter LGH), and, although it is not known whether its properties are typical of walls of galaxies, it has been used as a template in simulations of what could be detected at larger distances (LGH; RGH). With the aim of confirming the nature of the structures causing the redshift peaks in the direction of the north Galactic pole, as well as characterizing some of their properties, we have initiated a medium-deep redshift survey of 814 galaxies down to $B_J = 20$. This survey is centered at $\delta = 29\overset{\circ}{.}5$, and probes a larger right ascension range than BEKS. This longer baseline should allow us, in principle, to begin to explore the type of structures causing the BEKS peaks, e.g., walls or filaments.

[1] Visiting Astronomer, Kitt Peak National Observatory, National Optical Astronomy Observatories (NOAO), which is operated by the Association of Universities for Research in Astronomy, Inc. (AURA) under cooperative agreement with the National Science Foundation.

## 2. THE DATA

### 2.1. *Photometry and Astrometry of Plate Images*

The sample of galaxies was obtained from recent epoch Palomar Schmidt plates in blue ($J$) and red ($F$) scanned with the APM system (Kibblewhite et al. 1984) by N. Ellman and M. Irwin. A full description of the APM procedures for scanning and detection of objects has been presented by Maddox et al. (1990) and Infante & Pritchet (1992), so we shall only describe them briefly. Each plate is scanned twice, the first time to determine the sky level at each position on the plate, the second for the detection of images. For each detected image, a series of parameters including instrumental magnitudes, and several intensity-weighted moments of the light distribution and centroids, are then output to a catalog. The astrometric solution is derived by fitting the equatorial coordinates of detected PPM stars (Röser & Bastian 1988); the accuracy is usually better than 0″.5. An independent set of scans of the red plate was made with the NOAO PDS microdensitometer, and was then analyzed and classified using FOCAS (Jarvis & Tyson 1991; Valdes 1982). These three catalogs were matched and used the APM $J$ plate catalog as the primary source of coordinates. Instrumental magnitudes calculated by APM were transformed into $B_J$ and $R_F$ based on photographic photometry for the SA 57 region carried out by Kron (1980) with the modifications of Koo (1986). The rms error in this calibration is $\sim 0.2$ mag and a final calibration is currently under-

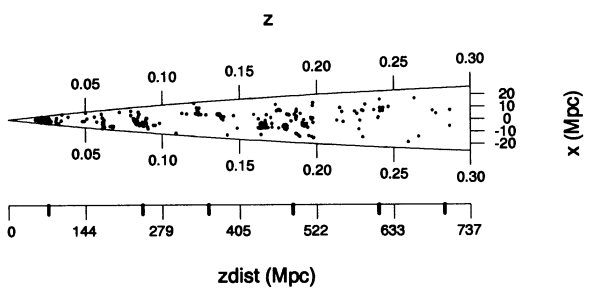


FIG. 1a

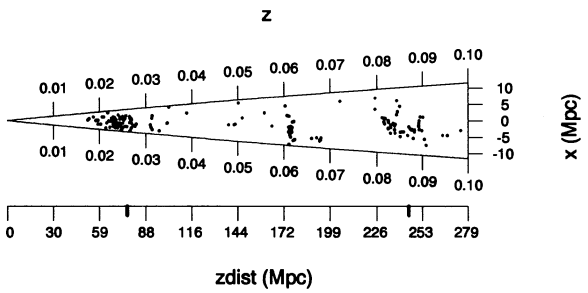


FIG. 1b

FIG. 1.—Spatial distribution of galaxies in redshift vs. co-moving transverse distances as derived from right ascension ($x$). The origin ($x = 0$) corresponds to R.A. = $13^h02^m$, and $x$ increases eastward. We also show rulings with co-moving radial coordinates so that the redshift can be more easily translated into distance. Panel (*a*) shows galaxies out to $z = 0.3$, while panel (*b*) is limited to $z \leq 0.1$ so that the nearer structures are magnified. The thicker tick marks denote the location of the BEKS peaks.

way using CCD photometry. The observational sample contains 814 galaxies brighter than $B_J = 20.0$ in a mini-slice limited by $12^h52^m$ and $13^h12^m$ in right ascension and 29°05′ and 29°54′ in declination (epoch 1950.0).

### 2.2. *Spectroscopy*

The spectroscopic observations were taken in 1992 February and 1993 February with the KPNO 4 m telescope using the HYDRA multifiber positioner (Barden et al. 1992) feeding a bench-mounted spectrograph. The spectral coverage on both runs was from 4100 to 8100 Å. The data were reduced following the standard IRAF[2] procedures to remove detector signatures while the spectra were extracted and mapped into wavelength using the DOHYDRA task written by F. Valdes. Radial velocities were measured with the RVSAO package (Kurtz et al. 1991), which provides a final velocity based on the combination of cross-correlation analysis with emission-line fits. By comparing redshifts of 17 galaxies that are in common with the sample of van Haarlem et al. (1993), we find $v_{our} - v_{vH} = -24 \pm 66$ km s$^{-1}$. From 13 galaxies in common with ZCAT (Huchra 1993), we get $v_{our} - v_{ZCAT} = -7 \pm 76$ km s$^{-1}$. Both results suggest that our measurements do not have a significant zero-point error, and that the external uncertainty is less than 100 km s$^{-1}$. However, these measurements come mainly from bright galaxies which have spectra with good signal-to-noise ratio (S/N), and until a more detailed comparison using lower S/N spectra is carried out, we will adopt a higher, and thus more conservative, estimate for the uncertainties of ~150 km s$^{-1}$ that corresponds to the resolution of the spectra. The total number of redshifts in this region to $B_J = 20$ is 327, of which 240 were measured in this survey, 69 from Koo et al. (1993), and the remaining from ZCAT. The sample presented in this work is only complete in redshifts to ~40% and is thus inadequate for any detailed statistical analysis. It does, however, already provide hints of the nature of the structures causing the peaks detected by BEKS.

## 3. ANALYSIS AND DISCUSSION

### 3.1. *Redshift Distribution*

The sample with available redshifts is shown in Figure 1, where we plot redshift against a comoving projected transverse distance derived from right ascension. The galaxy distribution displays a pattern similar to that seen in the shallower surveys where galaxies define thin but coherent structures separated by larger underdense regions. Figure 1 shows that the nearest four or five peaks of BEKS are caused by extended structures which have a rather irregular appearance, more like superclusters rather than walls of galaxies. The only structure with a wall-like appearance is the feature at $z \sim 0.06$, which does not correspond to a major peak in BEKS's deep sample.

The peak corresponding to the GW shows a velocity width of more than 5000 km s$^{-1}$ ($\Delta z \approx 0.017$), much larger than the median velocity dispersion of 230 km s$^{-1}$ estimated by RGH. This large velocity width is most likely due to the presence of the Coma cluster, which is less than 1° away from the southern edge of our survey.

The GW defines the near edge of an underdensity that extends to $z \sim 0.06$. This "void" has also been detected in the survey of van Haarlem et al. (1993) and the deep probes of Koo et al. (1993). The far edge of this void is traced by a small wall-like structure which occupies almost the full right ascension range of the survey, corresponding at this redshift to ~11 $h^{-1}$ Mpc. Although only two galaxies were detected by the BEKS deep probe, their nearby sample (Fig. 1*b* in BEKS) shows this structure to be more pronounced. This structure has also been detected by the Century Survey (Geller et al. 1994), which confirms its wall-like appearance. This concentration is followed by a small underdensity extending to $z \sim 0.08$. The far side of this void is delineated by another feature that occupies most of the right ascension range (~15 $h^{-1}$ Mpc) and reaches out to $z \approx 0.09$, a depth of ~30 $h^{-1}$ Mpc. This is the structure causing the second northern peak of BEKS. The distribution of galaxies suggests that this concentration could be formed by a wall inclined relative to the line of sight that intersects a more irregular distribution at $z = 0.09$. Beyond this structure is a large void that extends from $z \sim 0.10$ to $z \sim 0.15$ for negative $x$. This underdensity has a depth of ~100 $h^{-1}$ Mpc and width of at least 10 $h^{-1}$ Mpc. Its radial extent is slightly larger than the typical size of voids (80 $h^{-1}$ Mpc), although still smaller than the largest possible voids which would have a scale of 130 $h^{-1}$ Mpc (Blumenthal et al. 1992).

The third peak of BEKS's deep sample (see their Fig. 1*a*) corresponds to the clump at $z = 0.125$, located at $x \sim +10$ (~$13^h06^m$), which extends toward higher values of $x$ though with a lower density of points. This structure causes the second highest peak of the northern sample of BEKS and yet, this structure would be missed had the BEKS survey been carried out 1° or more to the west. The third BEKS peak also contains

[2] IRAF is distributed by NOAO, which is operated by AURA, Inc., under cooperative agreement with the National Science Foundation.

signal from a smaller structure that can be seen at $z \sim 0.14$, defining the nearer edge of an underdense region that reaches to $z \sim 0.16$. This underdensity is followed by a fairly complex concentration of galaxies between $z = 0.16$ and $z = 0.20$ that includes the cluster A1661 (Abell 1958). This very large concentration corresponds to the fourth BEKS peak. A large number of galaxies in this redshift range has been detected by Koo et al. (1993) in pencil-beam surveys at distances up to 3°.5 away from our survey, corresponding to projected distances of $\sim 20\ h^{-1}$ Mpc. This structure appears to enclose a small void at $z = 0.18$, $x = 0$. Our data suggest that A1661 at $12^h59^m.4$ + 29°21′ (Struble & Rood 1991) could be a superposition of two groups along the same line of sight, one at $z \approx 0.165$ and the other at $z \approx 0.19$. No distortion due to virial motions can be seen at the expected position for this object ($x = -3$), while the small elongation at $x \approx -7$ is caused by a group of galaxies to the west of the cataloged position of A1661. The last peak of BEKS we detect with any level of significance is the fifth one at $z = 0.24$ and is probably associated with a rich, red compact cluster of galaxies, II Zw 1305.4+2941, at the same redshift (Koo et al. 1988).

The redshift histogram is shown in Figure 2. The bin width of 0.005 in redshift is ~10 times larger than the estimated redshift uncertainties, so that the distribution is unaffected by the velocity errors. The alternation of peaks with underdensities is now more clearly seen, and most of the peaks in the northern sample of BEKS (represented by the dotted vertical lines) within our redshift limit are easily recognized. The greatest density contrast between the observed and expected samples occurs for the GW. The structures at $z \approx 0.06$, $z \approx 0.09$, and between $z = 0.16$ and $z = 0.20$ are all more than 3 $\sigma$ above the expected value if we assume Poisson statistics and adopt the curve normalized by the total number of redshifts.

### 3.2. *Velocity Widths of High-Density Regions*

We now make a preliminary estimate of some properties of the high-density peaks found in our mini-slice survey. For this, we counted galaxies in square cells (in right ascension and declination) with sides corresponding to the declination width of the survey (49′). The range of redshift was also restricted so that most of the galaxies belonging to the high-density structures would be included, while in the computation of statistics, only cells containing galaxies would be considered, i.e., empty cells were ignored when calculating mean values for the projected density and velocity dispersion (e.g., RGH). Because of the fixed angular size of the cells, their metric size varies with redshift. By means of Monte Carlo simulations, we tested if there would be a significant bias in the measurement of cell parameters, in particular the velocity dispersion, with redshift and consequently cell size. Using distributions where we simulated walls of galaxies at different distances (although always perpendicular to the line of sight), we could not detect any dependence.

Table 1 contains the relevant parameters for the first four peaks detected by BEKS, as well as for the wall-like structure at $z \sim 0.06$. For the GW, the density contrast between the number of detected galaxies and the expected homogeneous distribution normalized by the number of measured redshifts ($N_g/N_{nv}$) is 17. This value is comparable to the value found by LGH for a simulated probe (of 3°.15 by 1°.3) that contained the center of the Coma cluster. Additional evidence that the Coma cluster is being detected comes from the value we measure for the mean projected density of galaxies brighter than $-18.2 + 5 \log (h)$, which is $\Sigma \sim 6.6 \pm 2.5$ galaxies $h^2$ Mpc$^{-2}$, whereas LGH measured a mean projected density of $\Sigma \sim 0.3$ galaxy $h^2$ Mpc$^{-2}$ for the GW.

In the simulations to test the detection of walls, LGH would consider a structure as a significant density enhancement whenever the density contrast ($N_g/N_e$) was greater than 3. In our data, only two structures aside from the GW satisfy this condition (at $z \sim 0.06$ and $z \sim 0.09$), while the two remaining structures ($z \sim 0.12$ and $z \sim 0.16$) are below this limit, even though they are more than 3 $\sigma$ above the expected distribution when assuming Poisson statistics. The wall at $z \sim 0.06$ occupies a small velocity range, and because its velocity dispersion is smaller than the contribution due to measurement errors (Danese, De Zotti, & di Tullio 1980), we do not quote a $\sigma_v$ value. In contrast, the $z \sim 0.09$ peak has a large value of $\sigma_v$ partly because of its irregular shape, and partly because there might be an intersection of two structures as noted above. The table suggests that the $z \sim 0.12$ peak could be sparse, yet from Figure 1 we see that it is a fairly localized structure that occupies a larger volume than that of a typical cluster, but which does not show any obvious redshift distortions due to virial motions. Finally, the $z \sim 0.16$ peak exhibits a higher value for the velocity dispersion than found by RGH for the GW, which could be due to the combination of the somewhat irregular shape of this concentration and the presence of clusters.

The mean velocity dispersion for all structures is 497 ± 194 km s$^{-1}$. Excluding the GW this reduces marginally to 485 ± 236 km s$^{-1}$. If the $z = 0.16$ peak is also ignored, the

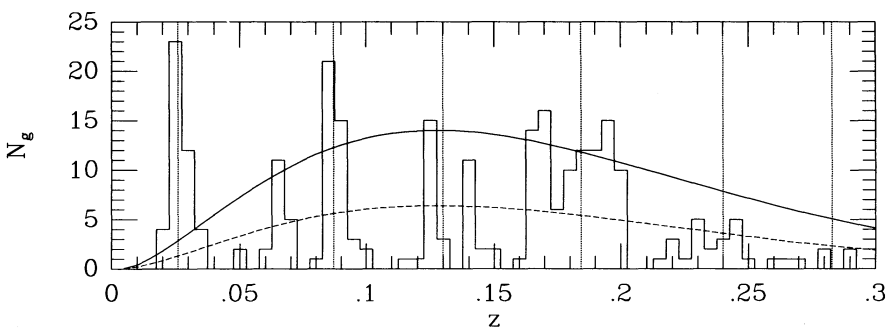


FIG. 2.—Histogram of galaxies in redshift bins of 0.005. The full line represents the expected distribution of galaxies for a homogeneous universe, assuming a Schechter luminosity function with parameters from Loveday et al. (1992): $M^* = -19.50 + 5 \log (h)$, $\alpha = -0.97$, and $\phi^* = 0.014\ h^3$. The dashed line is the same curve normalized by the total number of galaxies with redshifts. The peaks detected by BEKS are marked by dotted vertical lines.

TABLE 1

PARAMETERS OF HIGH DENSITY PEAKS

| $z$ Range (1) | $N_g$ (2) | $N_g/N_e$ (3) | $N_g/N_{nv}$ (4) | Cell Size $h^{-1}$ (Mpc) (5) | $\sigma_v$ (km s$^{-1}$) (6) | $N_{M\leq -18.2}$ (7) | Mean $\Sigma$ (galaxy $h^2$ Mpc$^{-2}$) (8) | Median $\Sigma$ (galaxy $h^2$ Mpc$^{-2}$) (9) |
|---|---|---|---|---|---|---|---|---|
| 0.020–0.030..... | 58 | 9.65 | 17.33 | 1.02 | 534 ± 272 | 35 | 6.7 ± 2.5 | 6.7 ± 1.9 |
| 0.060–0.065..... | 20 | 2.09 | 3.76 | 2.40 | ... | 11 | 0.5 ± 0.3 | 1.2 ± 0.4 |
| 0.081–0.091..... | 49 | 1.83 | 3.28 | 3.18 | 701 ± 438 | 39 | 0.8 ± 0.3 | 1.9 ± 0.7 |
| 0.120–0.130..... | 20 | 0.72 | 1.29 | 4.34 | 233 ± 164 | 18 | 0.5 ± 0.2 | 0.8 ± 0.4 |
| 0.160–0.172..... | 33 | 1.00 | 1.79 | 5.42 | 521 ± 143 | 33 | 0.3 ± 0.1 | 0.6 ± 0.2 |

Col. (1) Redshift range of cell. Col. (2) Number of galaxies in cells. Col. (3) Ratio of observed number of galaxies in cells to the expected distribution assuming a Schechter function with parameters of Loveday et al. 1992, integrated in bins of 0.001 in redshift. Col. (4) Ratio between the observed number of galaxies in cells to the expected distribution normalized by the total number of galaxies with redshifts. Col. (5) Metric size of square cells used for estimating surface densities; this corresponds to an angular size of 49′ given by the width of the survey in declination. Col. (6) Velocity dispersion and uncertainty estimated following Danese, De Zotti, & di Tullio 1980. Col. (7) Number of galaxies brighter than $M_J = -18.2$. Col. (8) Mean projected density of galaxies brighter than $M_J = -18.2$. Col. (9) Median projected density of galaxies brighter than $M_J = -18.2$.

mean $\sigma_v$ becomes 467 km s$^{-1}$ for the two remaining structures. The mean projected density excluding the GW (which represents a very deviant event in our sample) is 0.5 ± 0.3 galaxy $h^2$ Mpc$^{-2}$. These values are within about 1 $\sigma$ of those presented by RGH and LGH for the GW ($\sigma_v = 230$ km s$^{-1}$ and $\Sigma = 0.3$ galaxy $h^2$ Mpc$^{-2}$, respectively), and the implication is that the GW may not be an unusual structure. This conclusion, however, should be considered preliminary until the redshift sample becomes more complete.

## 4. CONCLUSIONS

We have undertaken a new moderately deep ($B \leq 20$) redshift survey of galaxies near the north Galactic pole. Among the 814 galaxies to this limit within a rectangular slice geometry of 4° by 49′, 327 have reliable redshifts, 240 of which are new. We confirm that four of the five nearest peaks of galaxies detected by BEKS in their redshift histogram are due to structures that extend in right ascension. The one exception at $z \sim 0.12$ appears to occupy only the eastern border of our field, so if the original BEKS survey had been undertaken only 1° or more to the west, no peak would have been seen. The distribution of galaxies has a pattern similar to that detected by shallower surveys (e.g., da Costa et al. 1994; Shectman et al. 1992). The appearance of our survey differs from that of Shuecker & Ott (1991), which reaches a comparable depth, in the sense that ours is not as smooth. This difference is probably due to the low spectral resolution of the slitless-grism redshifts used in that work, though their sampling rate is denser.

BEKS showed that their first peak is due to the Great Wall. In our survey, the GW represents a significant density enhancement, which reflects the presence of the Coma cluster, the center of which is about 1° away from the southern limit of our survey. The presence of galaxies from Coma is evident from the high value of the density contrast relative to a uniform sample and the projected density of galaxies. The remaining structures yield values for the velocity dispersion and mean surface density which are only somewhat higher than the values quoted by RGH for the Great Wall, suggesting that the GW is probably an average representative of walls of galaxies.

We would like to thank N. Reid for the loan of the POSS II plates; Ed Carder for assistance during PDS scans; S. Barden and T. Armandroff for their help during both HYDRA runs; and the KPNO staff for ensuring a very smooth operation. We also thank N. Ellman for sharing the APM catalogs and for helpful suggestions. The following grants have provided support to this project: CNPq 201036/90.8; NSF AST 9023178; and the US-Hungarian Science and Technology Grant J. F. No. 010/90. A. S. has been supported by NSF 90-20380, by OTKA in Hungary, an NSF-Hungary exchange grant in cosmology, and a grant from the Seaver Institute.

## REFERENCES

Abell, G. O. 1958, ApJS, 3, 211
Barden, S. C., Armandroff, T., Massey, P., Groves, L., Rudeen, A. C., Vaughnn, D., & Muller, G. 1992, ASP Conf. Ser. Vol. 37, Fiber Optics in Astronomy, ed. Peter M. Gray (San Francisco: ASP), 185
Blumenthal, G. R., da Costa, L. N., Goldwirth, D. S., Lecar, M., & Piran, T. 1992, ApJ, 388, 234
Broadhurst, T. J., Ellis, R. S., Koo, D. C., & Szalay, A. S. 1990, Nature, 343, 726 (BEKS)
da Costa, L. N., et al. 1988, ApJ, 327, 544
———. 1994, ApJ, 424, L1
Danese, L., De Zotti, G., & di Tullio, G. 1980, A&A, 82, 322
de Lapparent, V., Geller, M. J., & Huchra, J. P. 1991, ApJ, 369, 273 (LGH)
Geller, M. J., & Huchra, J. P. 1989, Science, 246, 897
Geller, M. J., Kurtz, M. J., Huchra, J. P., Fabricant, D. G., Schild, R., Thorstensen, J. R., & Wegner, G. 1994, in preparation
Huchra, J. P. 1993, private communication
Infante, L., & Pritchet, C. J. 1992, ApJS, 83, 237
Jarvis, J. F., & Tyson, J. A. 1981, AJ, 86, 476
Kibblewhite, E. J., Bridgeland, M. T., Bunclark, P., & Irwin, M. J. 1984, in Astronomical Microdensitometry Conference, NASA CP 2317, 277
Koo, D. C. 1986, ApJ, 311, 651
Koo, D. C., Ellman, N., Kron, R. G., Munn, J. A., Szalay, A. S., Broadhurst, T. J., & Ellis, R. S. 1993, ASP Conf. Ser. Vol. 51, Observational Cosmology Symposium, ed. G. Chincarini, A. Iovino, T. Maccacaro, & D. Maccagni (San Francisco: ASP), 112
Koo, D. C., Kron, R. G., Nanni, D., Trevese, D., & Vignato, A. 1988, ApJ, 333, 586
Kron, R. G. 1980, ApJS, 43, 305
Kurtz, M. J., Mink, D. J., Wyatt, W. F., Fabricant, D. G., Torres, G., Kriss, G. A., & Tonry, J. L. 1992, ASP Conf. Ser., Vol. 25, Proc. 1st Ann. Conf. Astronomical Data Analysis Software and Systems, ed. D. M. Worral, C. Biemesderfer, & J. Barnes (San Francisco: ASP), 432
Loveday, J., Peterson, B. A., Efstathiou, G., & Maddox, S. J. 1992, ApJ, 390, 338
Maddox, S. J., Sutherland, W. J., Efstathiou, G., & Loveday, J. 1990, MNRAS, 243, 692
Ramella, M., Geller, M. J., & Huchra, J. P. 1992, ApJ, 384, 396 (RGH)
Röser, S., & Bastian, U. 1988, A&AS, 74, 449
Schuecker, P., & Ott, H. A. 1991, ApJ, 378, L1
Shectman, S. A., Schechter, P. L., Oemler, A. A., Tucker, D., Kirshner, R. P., & Lin, H. 1992, in Clusters and Superclusters of Galaxies, ed. A. C. Fabian (Dordrecht: Kluwer), 351
Struble, M. F., & Rood, H. J. 1991, ApJS, 77, 363
Tully, R. B., Scaramella, R., Vettolani, G., & Zamorani, G. 1992, ApJ, 388, 9
van Haarlem, M. P., Cayón, L., de la Cruz, C. G., Martínez-González, E., & Rebolo, R. 1993, MNRAS, 264, 71
Valdes, F. 1982, Focas User's Manual (2d. ed.; Tucson: KPNO Computer Support Group)